Electronic Supplementary Material (ESI) for ChemComm.

Supporting Information

for

A General Scheme for Generating NMR Supersequences Combining High- and Low-Sensitivity Experiments

Jonathan R. J. Yong,[1] Ēriks Kupče,[2] Tim D. W. Claridge[1,*]

[1] *Chemistry Research Laboratory, Department of Chemistry, University of Oxford, Mansfield Road, Oxford OX1 3TA, United Kingdom*

[2] *Bruker UK Ltd, R&D, Coventry CV4 9GH, United Kingdom*

[*] tim.claridge@chem.ox.ac.uk

Contents

S1 Pulse programme description

This section presents a more detailed description of how the pulse programme works; this information is important to anybody seeking to use the pulse programmes given here (or anybody writing similar 'interleaved' experiments). We use the NOAH-4 A(B_N/B/S) experiment as an example here. In this experiment, the second module alternates between the ^{15}N HMBC (B_N), ^{13}C HMBC (B), and ^{13}C HSQC (S); the pulse programme is set up such that these three modules have fewer transients than the ADEQUATE (A). For every 8 transients of the ADEQUATE, 6, 1, and 1 transient(s) are recorded for the B_N, B, and S modules respectively.

An excerpt of the pulse programme is shown here and explained on the next page:

```
  "l3 = 0"      ; initialise loop counter
  "cnst51 = 8"  ; number of transients for ADEQUATE
  "cnst52 = 6"  ; number of transients for 15N HMBC
  "cnst53 = 1"  ; number of transients for 13C HMBC
  ; HSQC doesn't need a separate counter; it's just cnst51-cnst52-cnst53

2 d1

  ; run ADEQUATE
  goscnp ph30   ; record ADEQUATE FID

  if "l3 % cnst51 < cnst52" {
    ; transients 1 through 6: run 15N HMBC
    go=2 ph31
  }

  else {
  if "l3 % cnst51 < cnst52 + cnst53" {
    ; transient 7: run 13C HMBC
    go=2 ph31
  }

  else {
    ; transient 8: run 13C HSQC
    go=2 ph31   ; 'go' loops back to the label '2' a total of NS times
  }
  }

  1m iu3   ; increment loop counter
  if "l3 % cnst51 == 0" {
      ; increment t1 here
  }
  lo to 2 times x   ; see main text for description of x
```

Generally, interleaving is performed using modular arithmetic. A loop counter (`L3`) is used in order to keep track of how many transients have been recorded so far, and the value of this counter *modulo* 8 is used in order to determine which module to run in the second slot. Note that this is independent of the `NS` parameter in TopSpin. So, each t_1 increment of the ADEQUATE module is actually recorded 8 × `NS` times.

Of course, the values of `cnst51`, `cnst52`, and `cnst53` are not hardcoded as in the example above. By changing these numbers, the user can control the number of transients allocated to each module. In total, each t_1 increment of the ADEQUATE module is acquired `cnst51` × `NS` times; the ^{15}N HMBC is acquired `cnst52` × `NS` times; and so on. (For the final module (HSQC), there is no need to define an analogous `cnst54` because it simply 'uses up' all the remaining transients; thus, the HSQC is acquired a total of (`cnst51` − `cnst52` − `cnst53`) × `NS` times.)

Finally, t_1 is only incremented if we have completed a full cycle of 8 runs through the loop. Again, this is checked using modular arithmetic; every 8 loop iterations, `l3` will be a multiple of `cnst51`. The value of x in the last line corresponds to the total number of loop iterations which need to be made; thus, this value is equal to 8 times the number of desired t_1 increments.

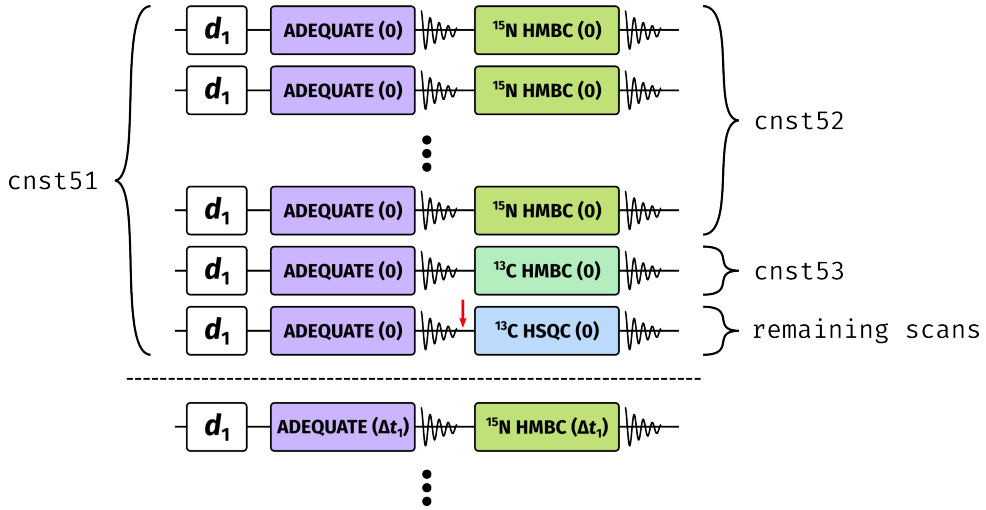

Figure S1: Diagram illustrating the practical implementation of the NOAH-4 A(B_N/B/S) supersequence. Numbers in parentheses refer to the value of t_1; the first increment is recorded with $t_1 = 0$ for all modules. d_1 represents a recovery delay. Each row is repeated `NS` times, during which phase cycling is performed; however, no phase cycling is performed *between* rows, even those which are identical (e.g. the first two rows). Since each row only consists of two horizontally concatenated modules, the `NBL` parameter is to be still set to 2. The red arrow indicates where DIPSI-2 mixing is inserted: this is discussed in Section S4.

It is worth pointing out at this point that, because of the way TopSpin increments pulse phase pointers, *phase cycling* (as defined by the phase tables in the pulse programme) is only carried out `NS` times. That is, although the ADEQUATE module is recorded `cnst51` × `NS` times, only a `NS`-step phase cycle is being used. With modern gradient-based coherence selection techniques,

this does not have a substantial impact on the data quality. (For example, the data in Figure 4 were recorded with NS=2 and are perfectly serviceable.) Nevertheless, it is always a good idea to make NS as large as possible, and always at least 2 to ensure suppression of axial peaks. As a concrete illustration, the two parameter sets below yield the same signal-to-noise for all modules, but parameter set 2 will have a longer (and presumably better) 4-step phase cycle.

	Parameter set 1, NS=2	Parameter set 2, NS=4
cnst51	12	6
cnst52	8	4
cnst53	2	1
cnst51 − cnst52 − cnst53	2	1

The parameter NBL should still be set to 2 for all of the supersequences shown in this work. The NBL parameter corresponds to the number of *sequentially* concatenated modules, which in all cases is only 2; the parallel modules play no role here. The value of TD1 should then be set to cnst51 × NBL × N_1, where N_1 is the desired number of t_1 increments (i.e. TD1 in a 'traditional' 2D experiment).

Finally, it should be noted that the if/else conditionals are evaluated only at runtime by the spectrometer. TopSpin does not calculate ahead of time when each interleaved module is run. This means that the TopSpin expt command (which shows the expected experimental duration) can yield (very slightly) inaccurate results.

S2 Pulse programme and processing script availability

The pulse programmes used in this work, along with all requisite processing scripts, can be downloaded from the Bruker User Library at https://www.bruker.com/protected/en/services/bruker-user-library.html, or equivalently, from GitHub at https://github.com/yongrenjie/abbs-paper/releases/tag/data. The zip archive contains further instructions on setting up the pulse programmes.

S3 NOAH-4 A(B_N/N/S) experiment

Since the ^{1}H–^{1}H NOESY uses the same ^{1}H$^{!C}$ magnetisation as ^{13}C HMBC so can be directly substituted in its place, leading to a NOAH-4 A(B_N/N/S) supersequence (Figure S3). This not only provides a wealth of through-bond correlations which aid in eludicating molecular constitution, but also furnishes through-space correlations for the determination of configuration or conformation. Depending on the molecular size and spectrometer frequency, the NOESY module may easily be replaced with a ROESY.

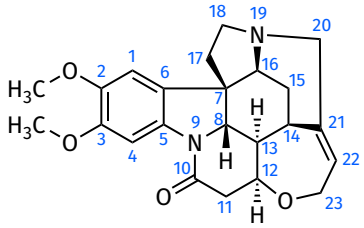

Figure S2: Structure of brucine.

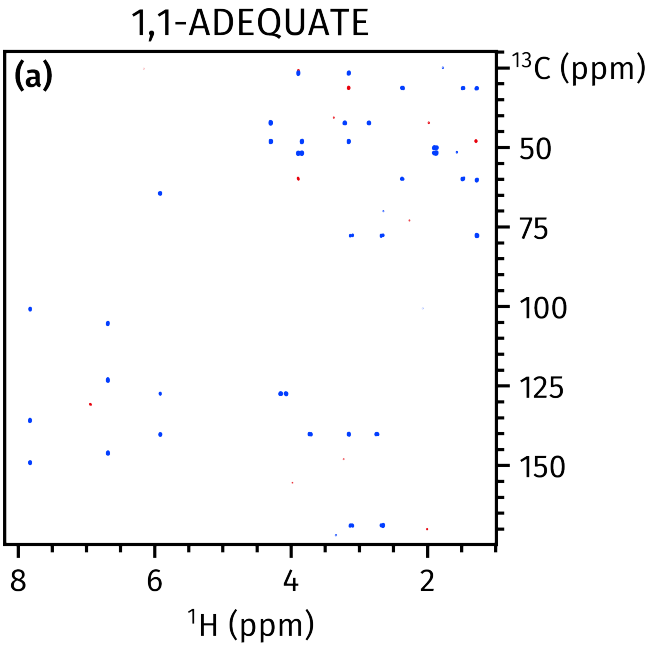
1,1-ADEQUATE
(a)
^{13}C (ppm)
50
75
100
125
150
8
6
4
2
^{1}H (ppm)

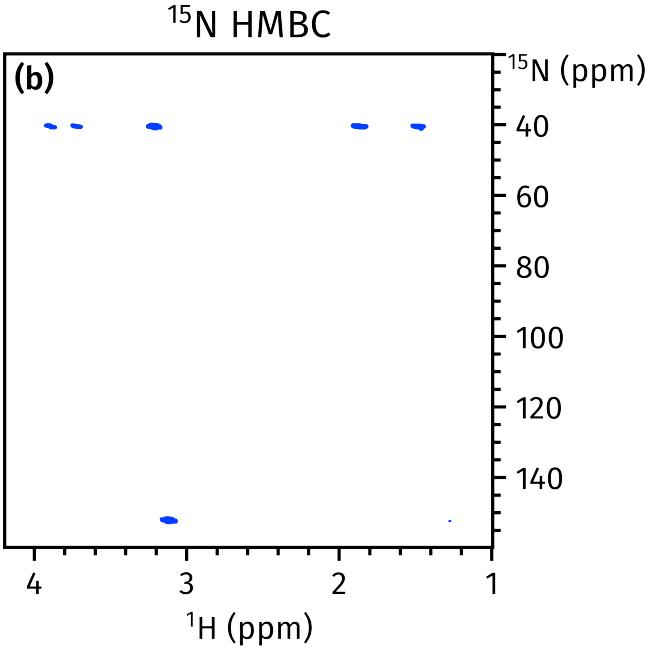
^{15}N HMBC
(b)
^{15}N (ppm)
40
60
80
100
120
140
4
3
2
1
^{1}H (ppm)

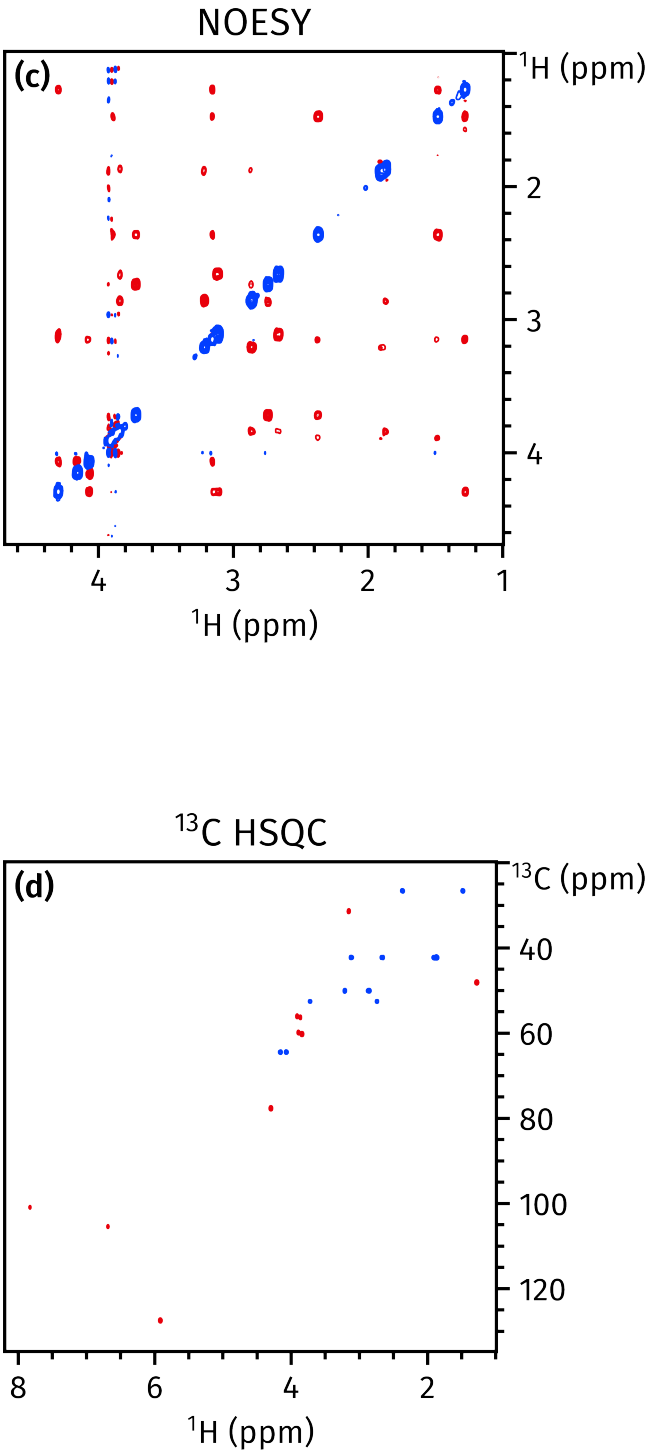

Figure S3: Spectra obtained from the NOAH-4 A(B_N/N/S) supersequence. **(a)** 1,1-ADEQUATE (16 transients). **(b)** ^{15}N HMBC (12 transients). **(c)** NOESY (2 transients, 800 ms mixing time). **(d)** ^{13}C HSQC (2 transients). Spectra were obtained on a 700 MHz Bruker AV III equipped with a TCI H/C/N cryoprobe; the sample used was 50 mM brucine in $CDCl_3$.

S4 NOAH-4 A(B_N/B/S) comparison with and without DIPSI

One additional feature of the NOAH-4 A(B_N/N/S), not described in the main text, concerns the fact that the ^{13}C HSQC module is placed immediately after the ADEQUATE (the second-last row in Figure S1). Both of these modules draw on the same $^1H^C$ magnetisation pool, and this generally causes the latter module (here HSQC) to suffer from sensitivity losses. Since the HSQC has a much greater intrinsic sensitivity compared to the ADEQUATE, this loss would in fact be tolerable.

In this experiment, we chose to also add a 35 ms period of isotropic DIPSI-2 mixing[1] immediately before the HSQC module (at the point marked with the red arrow in Figure S1). This effects $^1H^{!C}$ $\rightarrow$ $^1H^C$ magnetisation transfer, and has previously been demonstrated in ASAP[2–6] and NOAH[7] experiments. Through this, some of the lost $^1H^C$ magnetisation is replenished, leading to greater intensity in the HSQC (Figure S4). This mixing period does not need to be inserted prior to either of the ^{15}N or ^{13}C HMBC modules, as they do not use $^1H^C$ magnetisation. Figure S4 compares the results obtained with and without this DIPSI block.

The spectral quality in both cases is acceptable. However, the spectrum acquired without DIPSI mixing (Figure S4a) is weaker, which is more clearly shown in the projections onto the F_2 axes (Figure S4c). When DIPSI mixing is added, the average signal enhancement across all peaks in the HSQC is 88% (Figure S4). These observations are consistent with previous studies on NOAH supersequences containing two successive $^1H^C$ modules.[7]

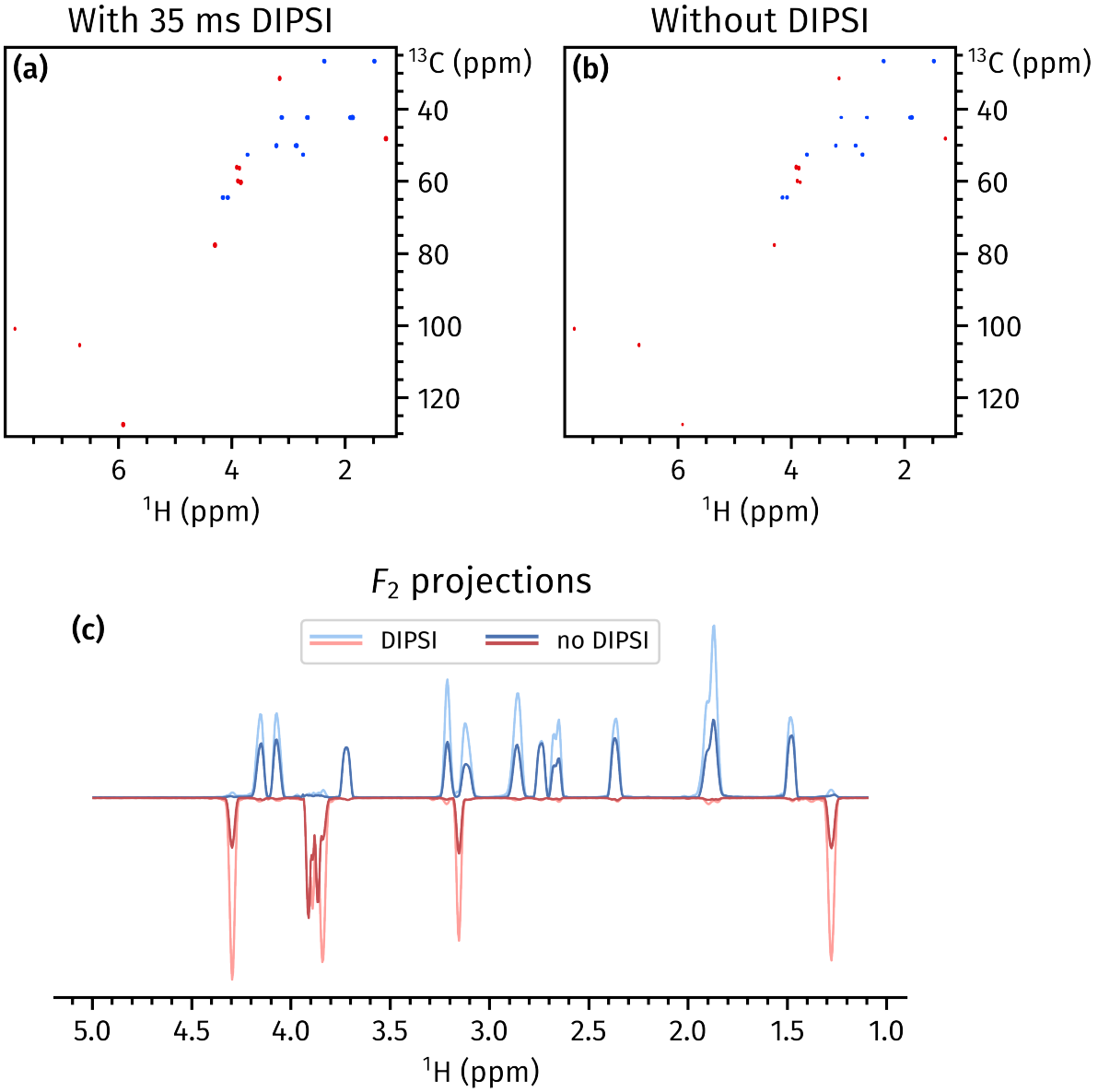

Figure S4: ^{13}C HSQC spectra obtained from the NOAH-4 A(B_N/B/S) experiment (Figure 1d). **(a)** With 35 ms DIPSI mixing between the ADEQUATE and ^{13}C HSQC modules (this spectrum is the same as in Figure 4d). **(b)** Without DIPSI mixing between the ADEQUATE and ^{13}C HSQC modules. **(c)** Projections of the spectra in (a) and (b) onto the F_2 axis. Spectra were obtained on a 700 MHz Bruker AV III equipped with a TCI H/C/N cryoprobe; the sample used was 50 mM brucine in $CDCl_3$.

S5 Spectra from NOAH-5 A(B_N/B/S_N^+/S)

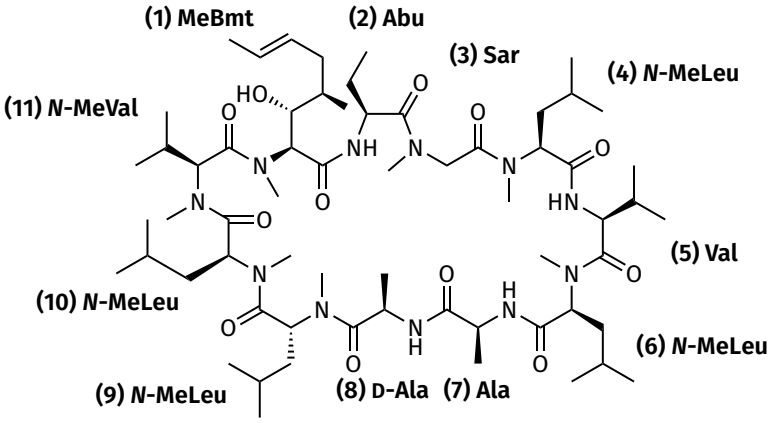

Figure S5: Structure of cyclosporin with residues numbered.

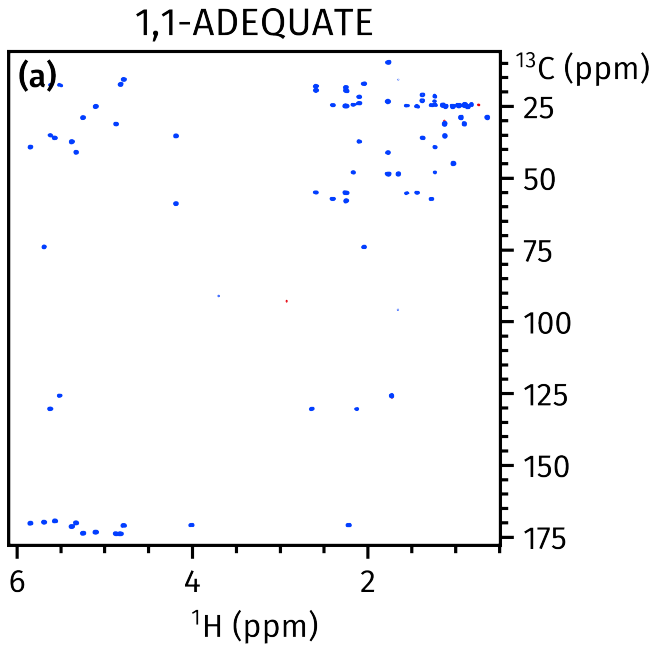

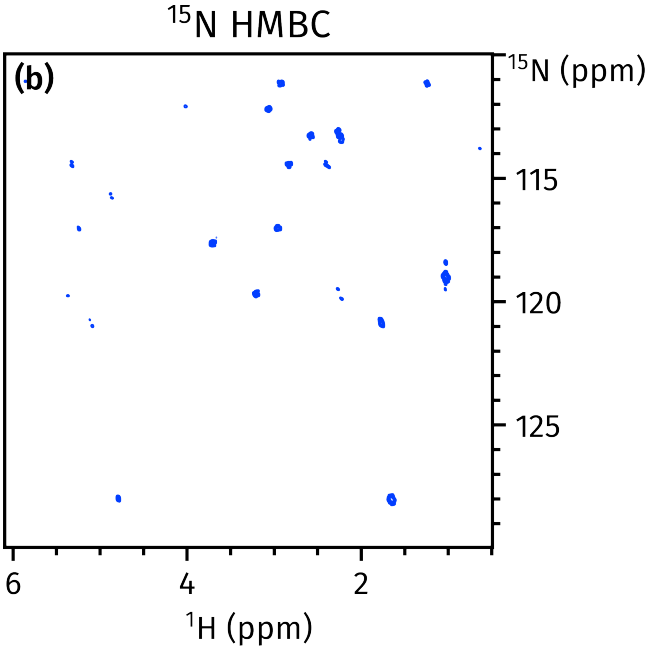
^{15}N HMBC
(b)
^{15}N (ppm)
115
120
125
6
4
2
^{1}H (ppm)

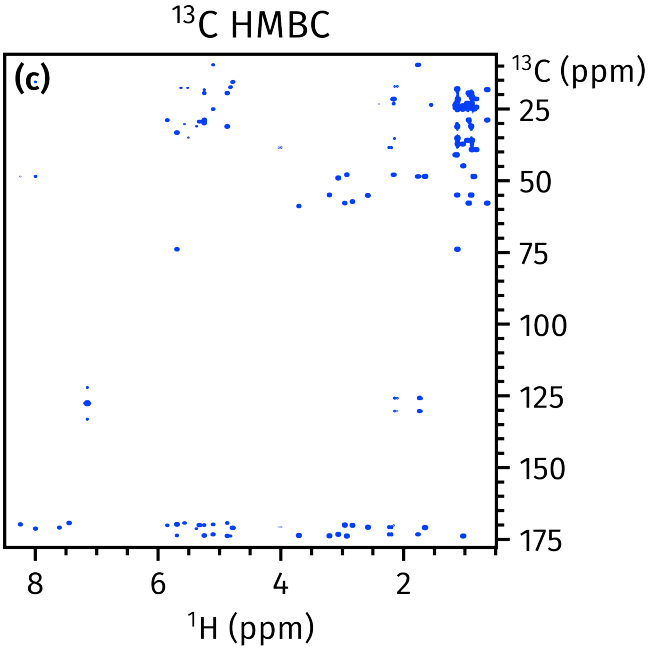
^{13}C HMBC
(c)
^{13}C (ppm)
25
50
75
100
125
150
175
8
6
4
2
^{1}H (ppm)

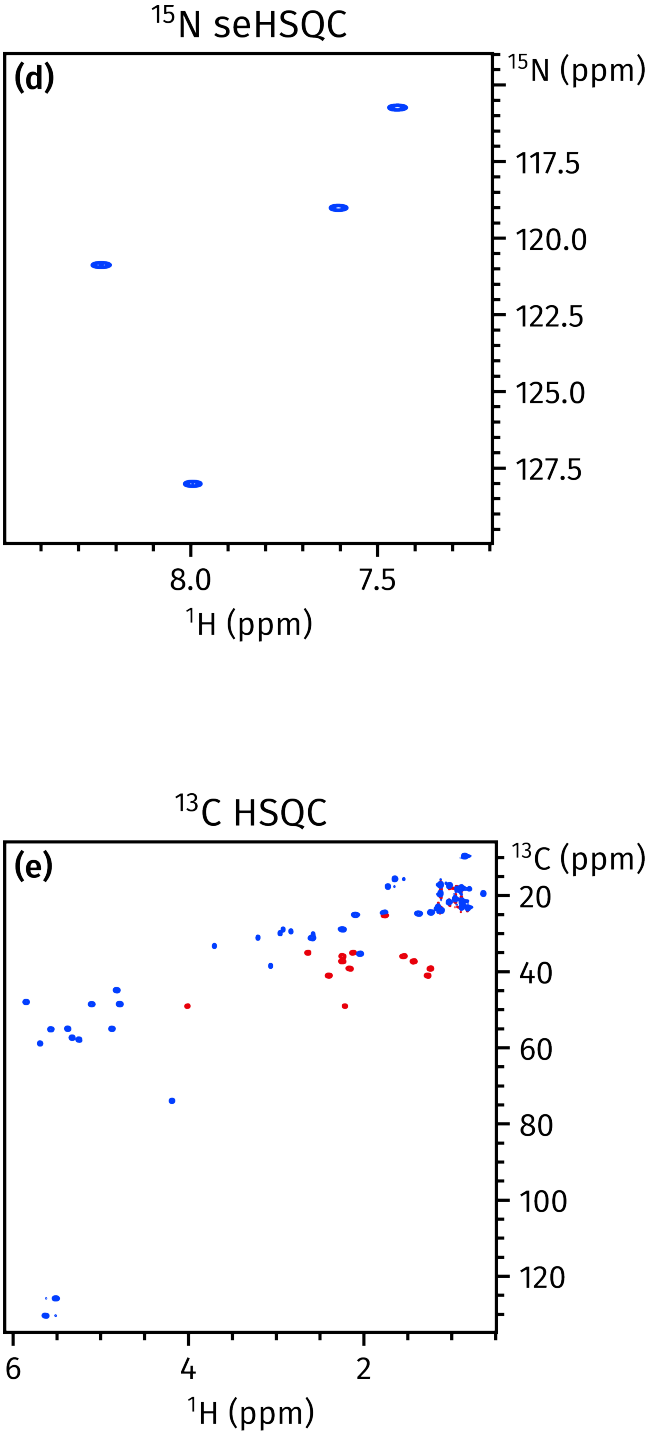

Figure S6: Spectra obtained from the NOAH-5 A(B_N/B/S_N^+/S) supersequence. All modules were recorded with 256 t_1 increments. **(a)** 1,1-ADEQUATE (16 transients). **(b)** ^{15}N HMBC (10 transients). **(c)** ^{13}C HMBC (2 transients). **(d)** ^{15}N sensitivity-enhanced HSQC (2 transients). **(e)** ^{13}C HSQC (2 transients). Spectra were obtained on a 700 MHz Bruker AV III equipped with a TCI H/C/N cryoprobe; the sample used was 50 mM cyclosporin A in C_6D_6.

S6 Covariance spectra from NOAH-5 A(B_N/B/S_N^+/S)

The heteronuclear spectra obtained from the NOAH-5 A(B_N/B/S_N^+/S) supersequence can be processed using indirect covariance processing[8–10] to yield other forms of correlation spectra. For example, the ^{15}N HMBC and ^{13}C HSQC can be used to generate ^{13}C–^{15}N correlation spectra (Figure S7a).[11–13] Furthermore, the ^{13}C HSQC and ADEQUATE experiments can be used to create ^{13}C–^{13}C one-bond correlation spectra (Figures S7b and S7c).[14,15] It should be further emphasised that all of the 'base' spectra used as the inputs here are obtained *in a single measurement* using either the NOAH-4 or NOAH-5 supersequences discussed above. A notable benefit of this is that t_1 for all modules are incremented simultaneously: this minimises the effects of temporal variations such as temperature drifts, which can lead to inaccurate peaks in covariance spectra.

In Figure S7c, the ^{13}C–^{13}C one-bond covariance spectrum has been subjected to a sign-preserving symmetrisation procedure. This is defined by replacing the intensity at each point $p(\Omega_1, \Omega_2)$ by

$$p(\Omega_1, \Omega_2) \rightarrow \operatorname{sgn}[p(\Omega_1, \Omega_2)] \cdot \min\left\{|p(\Omega_1, \Omega_2)|, |p(\Omega_2, \Omega_1)|\right\}. \tag{1}$$

Here, sgn p refers to the sign of p, or equivalently $p/|p|$ (for $p \neq 0$). The sgn p term ensures that the *sign* of each peak (and hence multiplicity information) is preserved, but the (absolute) intensities are symmetrised about the main diagonal, which suppresses artefactual responses arising from coincidental peak overlap.

It should be noted that such a procedure can only be safely carried out where peaks on both sides of the diagonals are expected. For a *true* ^{13}C–^{13}C correlation spectrum, this would be the case for all pairs of ^{13}C nuclei. However, the covariance spectrum shown in Figures S7b and S7c does not satisfy this: peaks at (Ω_1, Ω_2) are only observed if the carbon at Ω_2 is bonded to at least one proton. Thus, if the symmetrisation procedure is applied across the entire spectrum, correlations between quaternary and non-quaternary carbons (such as those in Figure S7b) will be lost. However, in the case of Figure S7c, the alkyl region of cyclosporin does not contain any quaternary carbons, allowing the symmetrisation to be safely carried out.

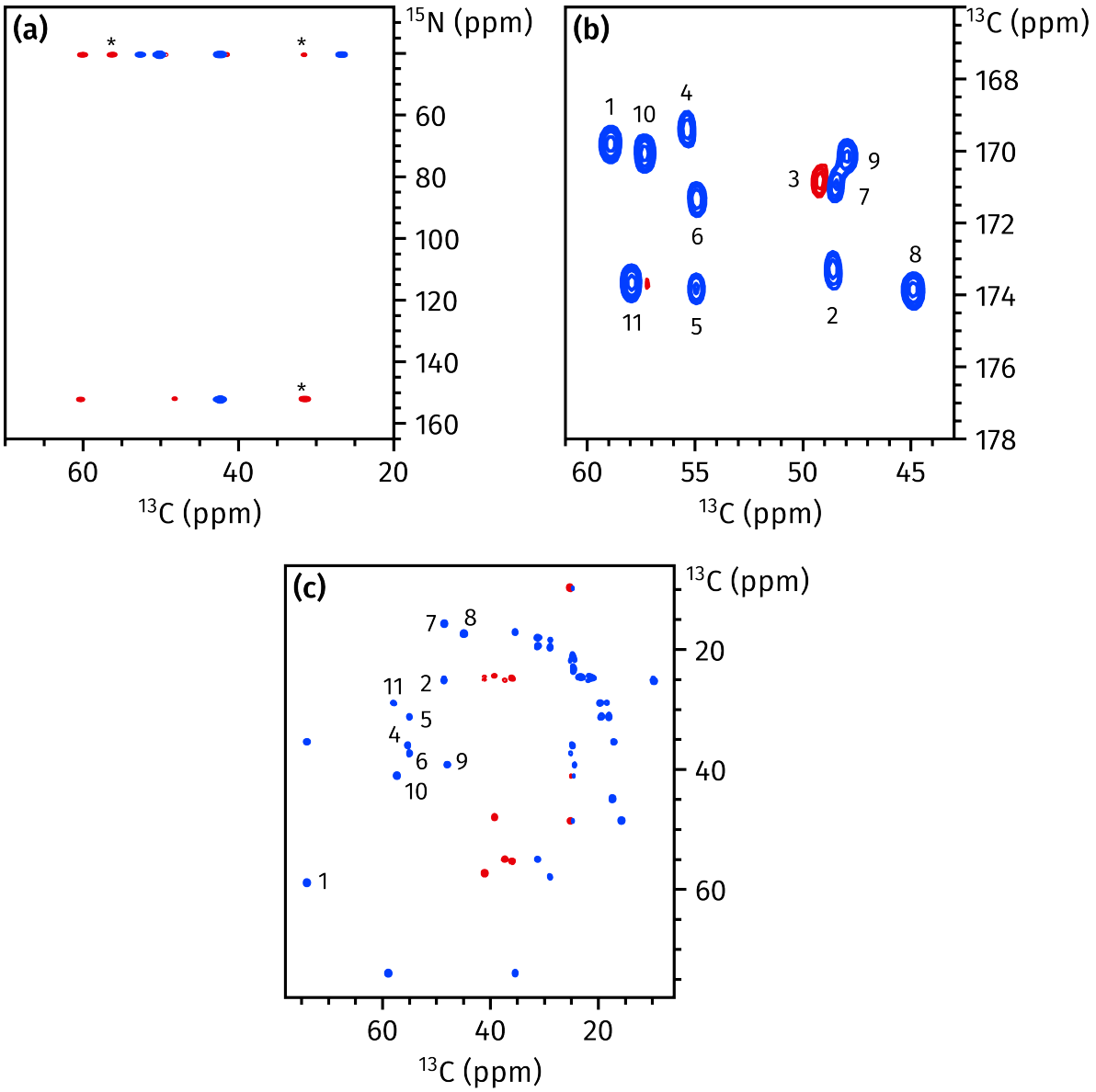

Figure S7: Spectra obtained through indirect covariance processing. In all cases the peak sign indicates carbon multiplicity; this information is contained in the multiplicity-edited ^{13}C HSQC spectrum and arises naturally during covariance processing. **(a)** ^{13}C–^{15}N correlation spectrum (containing both one- and multiple-bond correlations) obtained by processing the brucine ^{15}N HMBC and ^{13}C HSQC spectra (in Figures 4b and 4d) using unsymmetric indirect covariance. Some artefacts (arising from peak overlap in the ^{1}H dimension) are marked with asterisks. **(b–c)** Insets of ^{13}C–^{13}C one-bond correlation spectrum, obtained by processing the cyclosporin ADEQUATE and ^{13}C HSQC spectra (in Figures S6a and S6e) using generalised indirect covariance (λ = 0.5). The Cα–CO correlations, numbered by residue (see Figure S5), are shown in (b). Sidechain C−C correlations are shown in (c); only peaks corresponding to Cα–Cβ correlations are labelled. The inset in (c) has been further subjected to a sign-preserving symmetrisation procedure, which is described in the text.

S7 Software and raw data

All processing was carried out using TopSpin 3 or 4. Plots are generated in Python 3, using the `numpy`, `scipy`, and `penguins` libraries. The raw data used for this paper, as well as all scripts required for regenerating the plots, are available on GitHub: `https://github.com/yongrenjie/abbs-paper`.

S7.1 Covariance

The exact code used for covariance processing can be found in the `figures/covariance.py` script. A short overview is presented here. The following code excerpt calculates the unsymmetric indirect covariance between two spectra. Here, `penguins.read()` returns a `Dataset` object: the `rr` attribute of this is a two-dimensional `numpy` array corresponding to the doubly real part of the spectrum.

```
# Unsymmetric indirect covariance
import penguins as pg

spec1 = pg.read(path, expno1)
spec2 = pg.read(path, expno2)
cov = spec1.rr @ spec2.rr.T
```

Generalised indirect covariance is slightly more complicated, but follows directly from the procedure given in Snyder and Brüschweiler's work.[9]

```
# Generalised indirect covariance
import penguins as pg
import numpy as np
from scipy.linalg import fractional_matrix_power   # or just sqrtm

spec1 = pg.read(path, expno1)
spec2 = pg.read(path, expno2)
cov_lambda = 0.5

stacked = np.vstack((spec1.rr, spec2.rr))
cov_full = fractional_matrix_power(stacked @ stacked.T, cov_lambda)
# Figure out number of points in indirect dimensions of both spectra.
si1, si2 = spec1['si'][0], spec2['si'][0]
# `cov` is a block matrix, and we only want an off-diagonal block of it.
cov = np.real(cov_full[0:si1, si1:si1+si2)
```

Finally, this is the symmetrisation process specified in Equation (1). This assumes that the main diagonal of the *spectrum* corresponds to the main diagonal of the *matrix*, i.e. `m[i, i]` represents a point with the same chemical shift in both dimensions. The matrix `cov` calculated above satisfies this.

```
import numpy as np

def symmetrise_preserve_sign(m):
    smallest_amp = np.minimum(np.abs(m), np.abs(m).T)
    sign = np.sign(m)
    return sign * smallest_amp
```

References

(1) Shaka, A. J.; Lee, C. J.; Pines, A. Iterative schemes for bilinear operators; application to spin decoupling. *J. Magn. Reson.* **1988**, *77*, 274–293, DOI: 10.1016/0022-2364(88)90178-3.

(2) Kupče, E.; Freeman, R. Fast multidimensional NMR by polarization sharing. *Magn. Reson. Chem.* **2007**, *45*, 2–4, DOI: 10.1002/mrc.1931.

(3) Schulze-Sünninghausen, D.; Becker, J.; Luy, B. Rapid Heteronuclear Single Quantum Correlation NMR Spectra at Natural Abundance. *J. Am. Chem. Soc.* **2014**, *136*, 1242–1245, DOI: 10.1021/ja411588d.

(4) Schulze-Sünninghausen, D.; Becker, J.; Koos, M. R. M.; Luy, B. Improvements, extensions, and practical aspects of rapid ASAP-HSQC and ALSOFAST-HSQC pulse sequences for studying small molecules at natural abundance. *J. Magn. Reson.* **2017**, *281*, 151–161, DOI: 10.1016/j.jmr.2017.05.012.

(5) Koos, M. R. M.; Luy, B. Polarization recovery during ASAP and SOFAST/ALSOFAST-type experiments. *J. Magn. Reson.* **2019**, *300*, 61–75, DOI: 10.1016/j.jmr.2018.12.014.

(6) Becker, J.; Koos, M. R. M.; Schulze-Sünninghausen, D.; Luy, B. ASAP-HSQC-TOCSY for fast spin system identification and extraction of long-range couplings. *J. Magn. Reson.* **2019**, *300*, 76–83, DOI: 10.1016/j.jmr.2018.12.021.

(7) Yong, J. R. J.; Hansen, A. L.; Kupče, Ē.; Claridge, T. D. W. Increasing sensitivity and versatility in NMR supersequences with new HSQC-based modules. *J. Magn. Reson.* **2021**, *329*, 107027, DOI: 10.1016/j.jmr.2021.107027.

(8) Zhang, F.; Brüschweiler, R. Indirect Covariance NMR Spectroscopy. *J. Am. Chem. Soc.* **2004**, *126*, 13180–13181, DOI: 10.1021/ja047241h.

(9) Snyder, D. A.; Brüschweiler, R. Generalized Indirect Covariance NMR Formalism for Establishment of Multidimensional Spin Correlations. *J. Phys. Chem. A* **2009**, *113*, 12898–12903, DOI: 10.1021/jp9070168.

(10) Jaeger, M.; Aspers, R. L. E. G. Covariance NMR and Small Molecule Applications. *Annu. Rep. NMR Spectrosc.* **2014**, *83*, 271–349, DOI: 10.1016/B978-0-12-800183-7.00005-8.

(11) Kupče, E.; Freeman, R. Natural-abundance ^{15}N–^{13}C correlation spectra of vitamin B-12. *Magn. Reson. Chem.* **2007**, *45*, 103–105, DOI: 10.1002/mrc.1947.

(12) Martin, G. E.; Hilton, B. D.; Irish, P. A.; Blinov, K. A.; Williams, A. J. ^{13}C–^{15}N connectivity networks via unsymmetrical indirect covariance processing of ^{1}H–^{13}C HSQC and ^{1}H–^{15}N IMPEACH spectra. *J. Heterocyl. Chem.* **2007**, *44*, 1219–1222, DOI: 10.1002/jhet.5570440541.

(13) Martin, G. E.; Irish, P. A.; Hilton, B. D.; Blinov, K. A.; Williams, A. J. Utilizing unsymmetrical indirect covariance processing to define ^{15}N–^{13}C connectivity networks. *Magn. Reson. Chem.* **2007**, *45*, 624–627, DOI: 10.1002/mrc.2029.

(14) Martin, G. E.; Hilton, B. D.; Blinov, K. A. HSQC-ADEQUATE correlation: a new paradigm for establishing a molecular skeleton. *Magn. Reson. Chem.* **2011**, *49*, 248–252, DOI: 10.1002/mrc.2743.

(15) Martin, G. E.; Hilton, B. D.; Willcott III, M. R.; Blinov, K. A. HSQC-ADEQUATE: an investigation of data requirements. *Magn. Reson. Chem.* **2011**, *49*, 350–357, DOI: 10.1002/mrc.2757.